Aero-Hydrodynamics of an RS:X Olympic Racing Sailboard

Tim Gourlay and **Jon Martellotta**, Curtin University, Western Australia

SUMMARY

The RS:X Olympic sailboard is an all-round board designed to be raced in 4 to 25 knots of wind, and is an example of the current state-of-the-art in sailboard design. This board has been chosen as the specific example for an overview of sailboard aero-hydrodynamics. The current article brings together previous research on sailboard sail and fin lift, and applies it to the case of the RS:X sailboard. Measured sail camber and twist, as well as mast stiffness and deflection, are described for realistic upwind racing settings. The three-dimensional force and moment balance of an RS:X sailing upwind is investigated, in order to determine the limits on righting moment, sail lift and fin lift for different wind strengths. Finally a planing analysis is performed on the RS:X sailboard to calculate trim, wetted length and resistance.

1. INTRODUCTION

In this article we shall study the performance characteristics, rig tuning and force balance of a sailboard, specifically the current Olympic sailboard. Compared to keelboats and dinghies, little published research has been done on sailboards. This is unfortunate given the longevity of the sport, the high performance of racing and speed sailboards, and the fine force balance that is required for a sailboard to achieve controlled high speeds while riding on a small planing surface and single fin.

Both the sail and fin of a sailboard are standard foils, and can be analyzed using standard Computational Fluid Dynamics (CFD) methods. Avila (1992) used CFD and wind tunnel tests to study the flow around 2D sections of sailboard sails, focusing on lift coefficient and stall angle. It was found that combined panel method / boundary layer methods failed to produce converged solutions to flow around the sail at low angles of attack. Further analysis using full Navier-Stokes simulations and wind tunnel tests showed that a large recirculation zone exists on the windward side of the sail in this case. This separated flow field renders panel methods inaccurate in modelling flow around a sailboard sail, and requires a full Navier-Stokes analysis. Partida (1996) followed on from this work, using Navier-Stokes solvers to optimize sail section shapes, finding for example that an elliptical padded luff pocket ahead of the mast produces higher lift, less drag and higher stall angle.

The vertical distribution of sail lift is important for sailboards, particularly in strong winds, as the heeling moment able to be produced by the sailor has a limited maximum value depending on their height and body weight. Day (1996) found that maximum sail lift for a given heeling moment is achieved by having large twist in the sail. If practical, the optimum twist in strong winds would produce negative angle of attack near the top of the sail, so that the top of the sail would produce a windward heeling moment. However since this is not practical, it was found that the ideal twist for maximizing a sailboard's lift in strong winds (at constrained heeling moment) has zero angle of attack over the entire upper section of the sail, and positive angle of attack lower down.

Unlike Olympic dinghy classes, which have strict limitations on pumping the sail, sailboarders are permitted to pump the sail to generate additional lift. This is a near-sinusoidal transverse (and sometimes longitudinal) movement of the sail, similar to a bird flapping its wings. It is used on all points of sailing in light winds, and when accelerating out of tacks or gybes in medium and strong winds. It is easy to see the additional lift that such an action can produce when observing a bird taking flight. The sinusoidal transverse motion of a windsurfing sail has been studied using an unsteady Navier-Stokes code (Avila 1992). It was found that for a 2D sail section having a stall angle of 14º in steady flow, pumping the sail sinusoidally permitted attached flow on the leeward side at up to 18º unsteady angle of attack. Unsteady flow around a pumping sail has also been analyzed more recently for an RS:X sail (Wang et al. 2009). It has been shown (Castagna et al. 2007) that a high level of fitness is required in order to achieve sustained pumping of an RS:X sail in light winds.

Sailboard fins are often constructed using standard symmetrical NACA foil sections (Abbott & Von Doenhoff 1959), and the 3D effects of transverse bending, foil twist and partial stall are largely analogous to aeroplane wing theory. Due to the high angles of attack and high loads experienced by sailboard fins, twist

and its effect on stall are particularly important. The effects of fin rake and fin stiffness on twist and stalling characteristics were studied experimentally by Chiu et al. (1995). They found that fin twist is a fine balance between the torsional moments on each 2D section (which tend to increase the local angle of attack, since the centre of pressure is ahead of the shear centre), and rake, which has the opposite effect due to the torsional moment it induces on the fin as a whole. Stalling of sailboard fins is an important design consideration, as even the most modern fin designs are prone to stall. Stalling causes the tail of the board to spin suddenly away from the wind (known as "spinout"), and can occur when planing in any wind conditions. Stalling of an RS:X fin has been studied by Hansen (2011) using CFD software and wind tunnel tests. The process of spinout has also been found to be affected by ventilation of the fin (Swales et al. 1974, Broers et al. 1992).

2. THE RS:X SAILBOARD

The Neil Pryde RS:X is a one-design sailboard class, that was used for the Beijing 2008 Olympics and will shortly be used for the London 2012 Olympics. It is an "all-round" board and rig, designed to be raced in all wind conditions. The same equipment must be used throughout a regatta, including a 9.5m^2 sail for men and 8.5m^2 sail for women and youths.

Figure 1: RS:X board with men's 9.5m^2 rig

The board is fitted with a retractable centreboard and a fixed fin, enabling two distinctly different styles of upwind sailing. In light winds (up to 8 – 10 knots), the board is in displacement or marginal planing mode, with the centreboard fully down. In stronger winds, the board planes upwind on the fin, with the centreboard

fully retracted. For downwind sailing, the centreboard is normally fully retracted in all wind conditions, to minimize drag.

The sail of an RS:X is fully battened low-stretch monofilm, with camber inducers to lock the sail shape in, and a very stiff carbon mast and boom. The top of the sail is designed to twist off under high load.

In this article, we shall focus on upwind performance, and compare the mast bend, sail camber and leech twist, for different rig settings in both the displacement and planing modes. All sail analysis has been done using the men's 9.5m^2 sail and 5.2m mast.

2.1 CENTREBOARD DOWN AND RETRACTED UPWIND MODES

The RS:X sailboard has a considerably shorter length (2.86m) than the previous Mistral Olympic sailboard (3.72m). This gives it very different characteristics when operating in the displacement or marginal planing upwind mode, with the centreboard down.

The typical wave resistance peak (Newman 1992, p283) at a Froude number of 0.5 corresponds to a speed of 5.1 knots for the RS:X, taking the waterline length to be approximately equal to the board length in the displacement condition. An average sailor struggles to overcome this wave resistance peak in light winds, and hence often travels at or near the displacement "hull speed" (Killing 1998) of 4.1 knots. However top sailors, particularly in flat water, are able to pump the sail to accelerate the board through the wave resistance peak, and then cease pumping to achieve a steady speed of 6 – 8 knots (marginal planing). This has been observed through GPS analysis of race replays. Clearly, large gains can be made by operating on the right side of the wave resistance peak.

With the centreboard fully down, speeds above 8 knots are limited by the centreboard's drag, and by its excessive lift which renders the board uncontrollable. Once the wind strength is sufficient, higher upwind speeds are achieved by fully retracting the centreboard and bringing the board onto the plane.

A summary of representative displacement and planing scenarios for sailing upwind is presented in Table 1. The example board speeds and headings are based on GPS trials undertaken by the authors.

	Displacement or marginal planing, centreboard down	Planing, centreboard up
Wind range	< 8-10 knots	> 8-10 knots
Board speed range	3 – 8 knots	11 – 14 knots
Example wind strength	6.0 knots	12.0 knots
Example board speed	6.0 knots	12.0 knots
Example course relative to true wind	48º	58º
Velocity Made Good upwind	4.0 knots	6.4 knots
Apparent wind angle	24º	29º
Apparent wind speed	11.0 knots	21.0 knots

Table 1: Upwind scenarios, centreboard down or centreboard up

3. MAST FLEX AND BENDING STIFFNESS

RS:X masts are of two-piece construction, with an internal sleeve joining the top and bottom section, which allows them to come apart for transport and storage.

Eleven RS:X masts were tested to determine the flex characteristics under point loading. The masts were simply supported at a short distance of 255mm from each end, and a 31.2kg weight was suspended from the middle of the mast. The mast deflection was measured from a thin taut string attached to the ends of the mast.

Measured average deflections for the ¼, ½ and ¾ positions from the bottom of the mast are shown in Table 2. The error due to measurement inaccuracy and effect of string tension was estimated at ±2mm.

Mast position	¼	½	¾
Average deflection	125mm	201mm	149mm
Standard deviation	3.2mm	5.5mm	2.7mm

Table 2: Mast deflection under point loading

Examples of varying mast flex are shown in Table 3.

Mast serial #	Deflection at ¼, ½, ¾ locations	Characteristics
907334	124, 194, 146mm	Stiff bottom, stiff top
521494	125, 203, 151mm	Stiff bottom, flexible top
902412	131, 210, 152mm	Flexible bottom, flexible top

Table 3: Variations in mast deflection

The mast weights were also measured, to see if mast weight could be used as a measure of bending stiffness. The bending stiffness, or flexural rigidity *EI* is inversely proportional to the deflection under a given load (Timoshenko & Gere 1972). Similar testing with Laser dinghy aluminium masts (Martellotta 2010) has shown that for those masts the stiffness correlates very well with mast weight (correlation coefficient 0.66 over a sample of 15 masts). However, for the RS:X masts tested here, the correlation coefficient was found to be -0.12, indicating that heavier masts are not likely to be stiffer than lighter ones. For these masts, the amount of resin affects the weight directly, but the bending stiffness only slightly, so that variations in carbon/resin ratio result in little correlation between weight and bending stiffness.

4. STATIC RIG ANALYSIS

As mentioned in §2, the RS:X rig is quite rigid, with a fully battened sail and camber inducers to "lock in" the sail shape. Therefore, it is possible to analyze the rig on land without wind in the sail, and gain useful information about the shape of the rig.

4.1 RIG SETTINGS

The rig settings chosen here for analysis are from typical racing setups used by the authors. Constant settings are shown in Table 4 and variable settings shown in Table 5.

Mast extension	28cm
Boom extension	24cm
Boom height	Bottom of boom clamp 144cm above bottom of mast extension

Table 4: Constant rig settings used

Upwind settings, centreboard down		
Setting name	Sail tack	Sail clew
D24O20	4cm off block-to-block	4cm off block-to-block
D24O22	4cm off block-to-block	2cm off block-to-block
Upwind settings, centreboard retracted		
Setting name	Sail tack	Sail clew
D27O22	1cm off block-to-block	2cm off block-to-block
D27O24	1cm off block-to-block	0cm off block-to-block

Table 5: Variable rig settings for different conditions

The variable rig settings are named in terms of the downhaul and outhaul, e.g. D24 corresponds to 28cm mast extension with 4cm gap to the sail tack, while O22 corresponds to 24cm boom extension with 2cm gap to the sail clew.

We see that in non-planing conditions, minimal downhaul and outhaul are applied, in order to achieve a full sail with a tight leech. In planing conditions, considerably more downhaul is applied, to twist off the top of the sail and lower the centre of effort. As seen in Table 1, the planing upwind scenario with centreboard retracted entails a much higher apparent wind speed, as well as a larger apparent wind angle.

4.2 FORE-AFT MAST BEND

The RS:X sail has a curved luff pocket, such that considerable fore-aft mast bend is induced when rigging the sail. Tests were undertaken to study the fore-aft mast bend of the rigged sail, and how this varies with sail settings.

SailTool software, developed at Curtin University, was used to find the fore-aft mast bend by digitizing a side-on image of the rigged sail. An example digitized image is shown in Figure 2.

Figure 2: Digitized SailTool image of fore-aft mast bend

Firstly, a comparison was made of the differences in fore-aft mast bend caused by rigging the same sail with the same downhaul and outhaul, on masts of different stiffness. It was found that despite the significant variation in mast stiffness, the differences in fore-aft mast bend were negligible, and lay within the measurement error. In essence, the fore-aft mast bend in a tensioned sail is governed by the shape of the sail and the downhaul and outhaul, rather than the mast stiffness. Similarly, the sail camber profile (to be discussed subsequently) was found to be unaffected by the mast stiffness, when using the same downhaul and outhaul settings.

Therefore all mast and sail analysis was subsequently done using a single mast, which is the first mast shown in Table 3. However it must be recognized that although mast stiffness may not noticeably affect static sail shape, it is expected to affect transverse mast bend under load and hence loaded sail shape, and it will also affect the natural bending oscillation frequency and hence the dynamic sail pumping behaviour.

Fore-aft mast bend profiles are shown in Figure 3, for the different rig settings described in Table 5. The 31.2kg midpoint loading bend profile (from Table 2) is also included for comparison. Note that the base-to-tip chord length is slightly different in each case, as the rigged sail has a 28cm mast extension fitted, while the midpoint loading test was done for the mast alone.

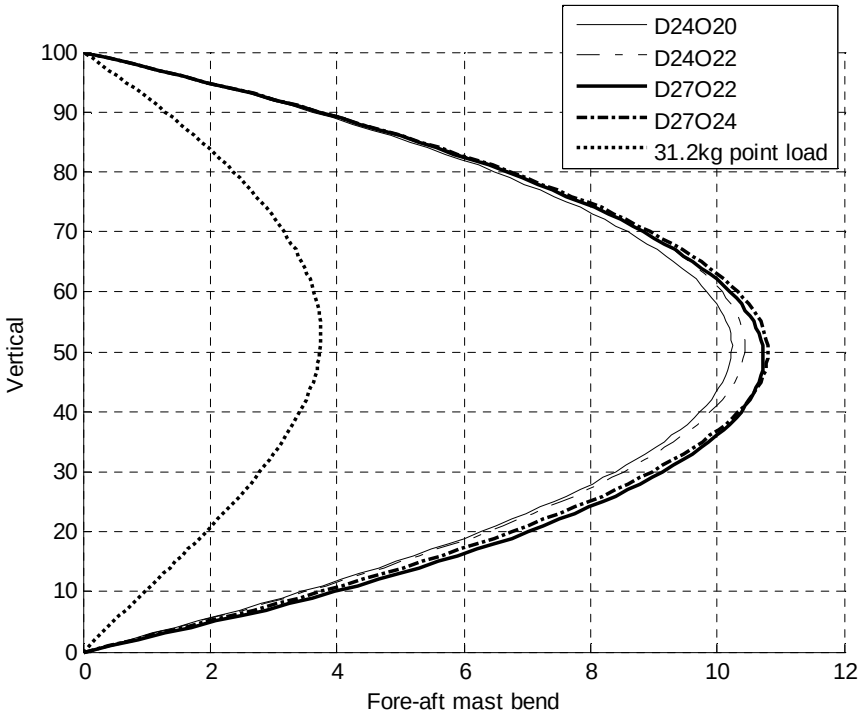

Figure 3: Fore-aft mast bend profiles for different rig settings (plotted as % of base-to-tip chord length)

We see that increased outhaul has a "bow and arrow" effect, bending the whole mast. Increased downhaul also bends the whole mast, but particularly the lower section, by exerting tension along the luff sleeve.

The mast bend of the rigged sail has up to 10.8% camber, while the 31.2kg point loaded mast has 3.7% camber. This indicates the extreme bending moment in a rigged RS:X mast.

4.3 DOWNHAUL TENSION

In order to achieve the mast bend profiles described in §4.2, high downhaul tension is required for the RS:X sail. Sailors use an adjustable downhaul system with a 32:1 purchase. Using a tension meter on the tail of this system allows the total tension at the sail tack to be measured. Results are shown in Table 6 (without wind in the sail).

Downhaul setting	Gap between sail tack and pulley	Total downhaul tension
D23	5cm	560N
D24	4cm	570N
D25	3cm	1000N
D26	2cm	1200N
D27	1cm	1310N
D28	0cm (block-to-block)	1480N

Table 6: Downhaul tension for different rig settings

4.4 SAIL TWIST

The top of an RS:X sail is designed to twist off when downhaul tension is applied, decreasing the wind angle of attack on the upper section, lowering the centre of effort and hence maximizing sail lift (Day 1996). The measured static leech twist angles (with the sail lying horizontal under gravity) are shown in Table 7. These are defined as the angle between the chord line of the sail and the line of the boom. Battens are numbered from the top down, as per the RS:X convention.

	D24O20	D24O22	D27O22	D27O24
Batten 1	4.8	3.5	7.0	6.8
Batten 2	5.1	3.7	7.6	7.3
Batten 3	3.5	2.1	4.6	3.9
Batten 4	2.5	1.6	2.4	1.4
Batten 5	1.5	1.0	1.3	0.6

Table 7: Twist angle (degrees) for different rig settings

4.5 SAIL CAMBER

Sail camber profiles were measured at battens 1-7, using SailTool to analyze a digital image taken from the top of the sail, with the sail in the horizontal position on land. Measured camber and draft are shown in Table 8 and Table 9.

	D24O20	D24O22	D27O22	D27O24
Batten 1	0.6	0.7	0.2	0.4
Batten 2	1.5	1.3	0.8	0.9
Batten 3	3.6	3.0	3.0	2.2
Batten 4	5.7	5.3	4.9	4.0
Batten 5	8.4	7.5	7.7	6.8
Batten 6	9.7	9.2	9.2	8.7
Batten 7	10.5	10.1	10.0	9.4

Table 8: Maximum camber (as percent of chord)

	D24O20	D24O22	D27O22	D27O24
Batten 1	11	9	50	50
Batten 2	20	12	12	10
Batten 3	21	22	29	16
Batten 4	27	25	23	19
Batten 5	25	23	26	30
Batten 6	27	29	30	28
Batten 7	32	35	27	32

Table 9: Draft, or position of maximum camber (as percent of chord from leading edge)

5. FORCES ACTING ON AN RS:X SAILBOARD

The balance of external forces on a sailboard is similar to that on a dinghy or yacht (Marchaj 1979). However, forces between the rig and hull are quite different, due to the universal joint which can sustain linear forces but no rotational moments. This means that the reaction force between the board and the sailor's feet must be such that the net moments about the universal joint are zero.

5.1 COORDINATE SYSTEM

The coordinate system chosen has its origin at the base of the universal joint which connects the rig to the board. The longitudinal coordinate x is positive forward, the transverse coordinate y is positive to port, and the vertical coordinate z is positive upwards.

5.2 HEEL, TRANSVERSE FORCE AND VERTICAL FORCE

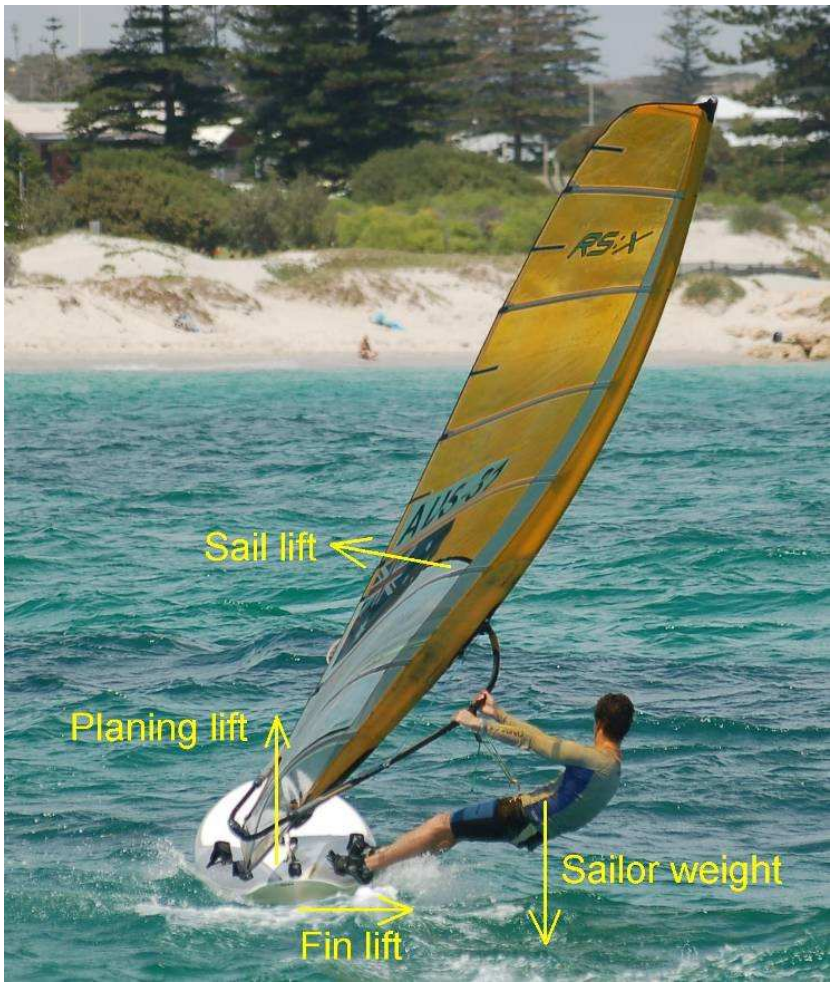

Figure 4: Planing upwind: main transverse and vertical forces

Figure 4 shows an RS:X planing upwind with centreboard retracted, together with the major forces acting in the transverse and vertical directions (*yz* plane). A diagram of the centreboard-down upwind stance is shown in Figure 5, together with the relevant forces in more detail.

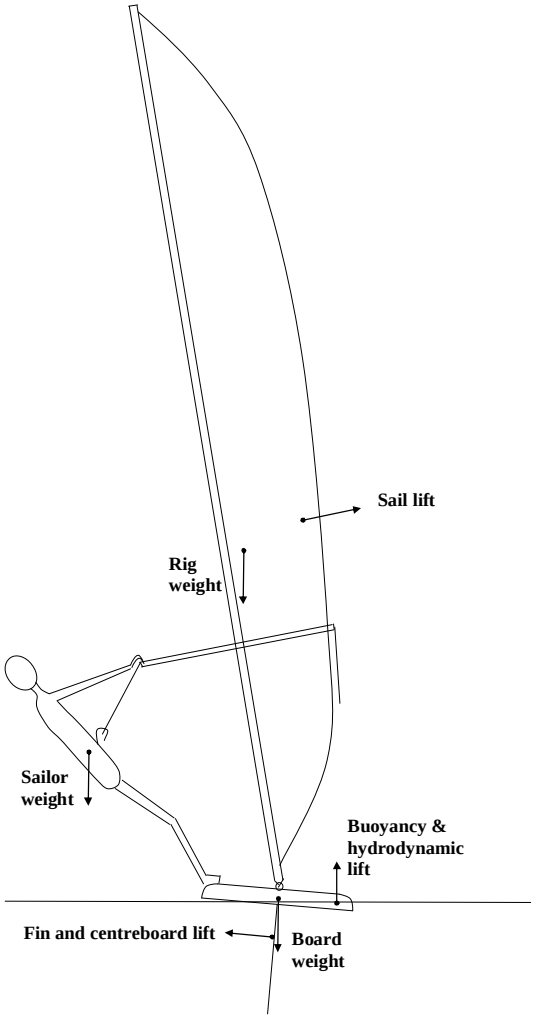

Figure 5: Sailing upwind with centreboard down: transverse and vertical forces

The heeling moment produced by the sail lift, fin lift and centreboard lift, is counteracted by a heel restoring moment from the rider's weight, rig weight, and hull buoyancy.

The aerodynamic lift force produced by the sail is balanced against the hydrodynamic lift force produced by the fin (and centreboard if unretracted). The board also produces a small transverse lift force through its sharp rail shape.

5.3 YAW AND HORIZONTAL FORCES

The net aerodynamic and hydrodynamic forces acting in the (*xy*) plane are shown in Figure 6.

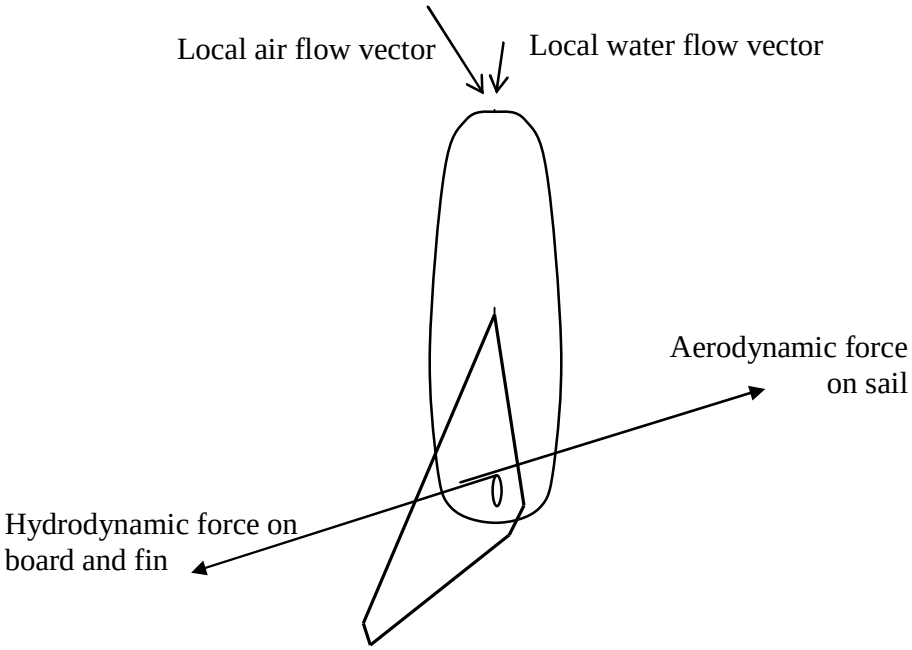

Figure 6: Aerodynamic and hydrodynamic force balance in horizontal (*xy*) plane

Yaw balance for a sailboard requires the sail to be held in such a position that the aero- and hydro-dynamic forces are co-linear in the (*xy*) plane.

When viewed in profile, the aero- and hydro-dynamic lift centres are at approximately the same longitudinal position, as shown in Figure 7.

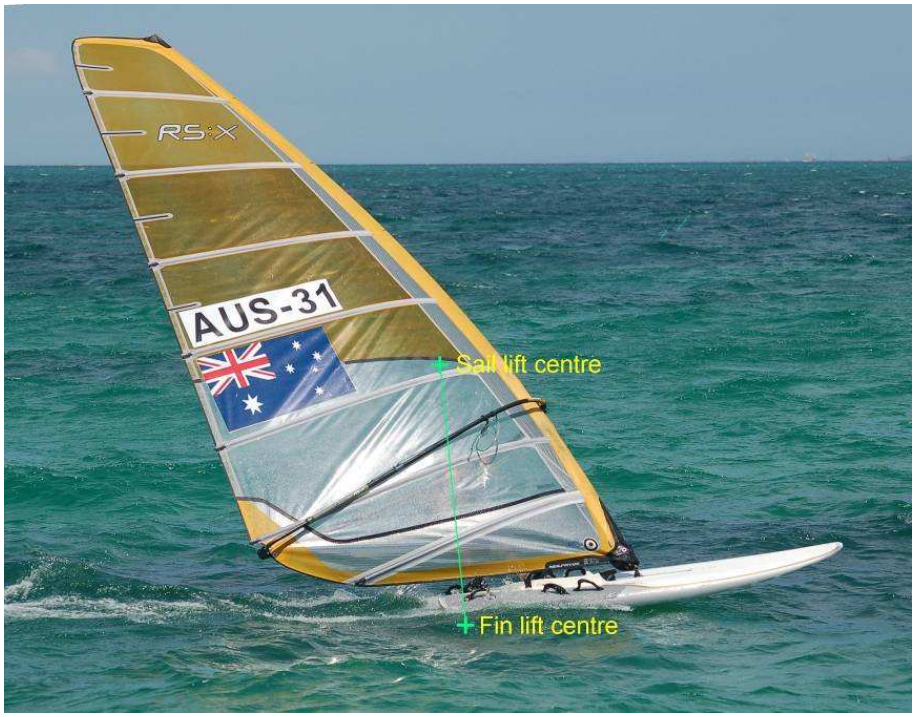

Figure 7: Yaw balance while planing upwind - sail and fin lift centres at similar longitudinal position

Steering the board is achieved by moving the rig forward (to steer away from the wind) or moving the rig aft (to steer toward the wind). When planing, the board can also be steered like a surfboard, by heeling the board to windward or leeward.

5.4 PITCH BALANCE

When sailing upwind with the centreboard down, the hull is in displacement or marginal planing mode (§2.1) with waterline length close to the board length, and a large pitch restoring moment due to hull buoyancy. However when planing with the centreboard retracted, the wetted length is much shorter and pitch balance becomes more important. Forces contributing to pitch balance are shown in Figure 8.

Figure 8: Planing upwind - pitch moment balance

6. HULL AND RIG FORCE LIMITATIONS

6.1 SAILOR AND RIG WEIGHT

Castagna (2007) performed a physiological analysis on ten top RS:X competitors, finding that they had an average height of 1.80m and average weight of 72.5kg. We shall use these values to represent a "standard" top RS:X competitor. Taking the centre of gravity height of an average male to be 0.57 times his height (Luciani 1913), this equates to the centre of gravity being 1.03m above the bottom of the feet. We shall also allow for 5kg of wet clothing, as class rules (ISAF 2011) dictate a maximum wet clothing weight of 6kg. This brings the standard sailor plus clothing weight to 77.5kg.

The maximum possible heeling moment due to the sailor's weight is achieved when the legs are straight and the body is nearly horizontal. However, as the body comes close to horizontal, the rig angle to windward must also increase, since the boom must be held at arm's length or closer (see Figure 4 and Figure 5). A large proportion of the sailor's heeling moment is transferred to the rig through the use of a seat harness, with harness line tension having been measured at around half the sailor's weight (Walls & Gale 2001).

In order to keep an efficient sail shape (with the rig reasonably upright), as well as to avoid the sailor's body hitting the waves and to provide some downward pressure on the windward side of the board, the sailor's body is generally kept at least $20^o - 30^o$ above horizontal (see Figure 4). Using a minimum angle of 20^o above the horizontal, the sailor's centre of gravity is then a transverse distance of 0.97m from the edge of the board. With centreboard down, in the forward footstraps, the heel position is 0.45m from the centreline, while with centreboard up, the rear footstrap heel position is 0.31m from the centreline.

Therefore the maximum heeling moment the standard sailor's weight can exert about the universal joint is 1080Nm with the centreboard down (and standing near the wide part of the board), and 970Nm with the centreboard up (standing in the rear footstraps).

The weight of the rig, when leaned to windward, also produces a heeling moment. The rig has a dry weight of 12.5kg, with centre of gravity 2.3m above the base of the universal joint. The maximum heel to windward of the rig is around 30º (see Figure 4), which produces a heeling moment of 240Nm.

6.2 FIN AND CENTREBOARD LIFT

When sailing upwind with the centreboard retracted, the fin of an RS:X is under intense loading, and prone to stall occasionally (the "spinout" problem described in §1). The maximum lift produced by the fin may be estimated based on wind tunnel results (Broers et al. 1992) for a similar fin planform. In that case, it was found that a maximum lift coefficient of 0.72 was achieved before the fin stalled. Using this same lift coefficient allows us to estimate the maximum lift of the RS:X fin and centreboard, for the upwind scenarios described in Table 1. The profile area of the fin is 0.063m^2, while that of the centreboard is 0.12m^2.

6.3 HULL BUOYANCY MOMENT

When the board heels to leeward with the centreboard down, an additional righting moment is exerted about the universal joint. The maximum righting moment due to buoyancy may be estimated as follows:
- representative total hull, rig and crew weight 110kg (hull and appendages 19.5kg, rig 12.5kg, sailor plus clothing 77.5kg)
- with centreboard down (non-planing), maximum outboard movement of centre of buoyancy estimated as 0.3m from centreline, giving 330Nm righting moment about the universal joint.

When planing, the board is kept fairly flat, and the hull buoyancy righting moment is small.

6.4 SAIL LIFT

The RS:X 9.5m^2 sail has an effective aspect ratio of 6.4. Based on limited wind tunnel tests of dinghy and yacht sails (Marchaj 1979, p444,550) we can estimate its maximum lift coefficient as approximately 1.4.

6.5 COMBINED EXTERNAL TRANSVERSE FORCES AND HEELING MOMENTS

Estimated maximum values of transverse forces are shown in Table 10, for the centreboard down and centreboard retracted scenarios described in Table 1.

	Displacement or marginal planing, centreboard down	Planing, centreboard up
Fin lift	-220N	-1080N
Centreboard lift	-420N	0
Sail lift	260N	930N

Table 10: Estimated maximum values of transverse forces (positive to leeward) before stall

We see that with the centreboard down, the maximum lift produced by the fin and centreboard is much greater than that produced by the sail, so that the sail is likely to stall before the fin and centreboard. With the centreboard up, the maximum lift produced by the sail and fin are similar, so that the sail and fin have similar likelihood of stalling.

Estimated maximum heeling and righting moments are shown in Table 11, for the centreboard down and centreboard retracted scenarios described in Table 1. For the centreboard and fin, the centres of lift are approximated by the geometric centres, which are 0.35m and 0.28m beneath the bottom of the board respectively. The thickness of the board is 0.13m at the universal joint. The sail's centre of lift is approximated by its centre of gravity, i.e. 2.3m above the base of the universal joint.

	Displacement or marginal planing, centreboard down	Planing, centreboard up
Sailor and rig weight moment	-1320Nm	-1210Nm
Hull buoyancy moment	-330Nm	0Nm
Fin lift moment (at stall)	90Nm	440Nm
Centreboard lift moment (at stall)	200Nm	0Nm
Sail lift moment (at stall)	600Nm	2100Nm

Table 11: Estimated maximum values of heeling moment about universal joint (positive heeling to leeward)

For the centreboard down upwind scenario given in Table 1, we see that the maximum righting moment produced by the sailor and rig weight, is larger than the maximum heeling moment produced by the fin, centreboard and sail. Therefore the sailor can easily achieve the required righting moment without having to lean excessively to windward or heel the board to leeward. Nevertheless, most sailors prefer to have a moderate leeward heel when sailing with centreboard down, to decrease the wetted area of the board and hence the viscous resistance.

For the planing (centreboard retracted) scenario, the maximum righting moment produced by the sailor and rig weight, is much *smaller* than the maximum heeling moment produced by the fin and sail. Therefore the sailor's righting moment is the major constraint while planing upwind, and the sailor must achieve the maximum possible extension to windward, to maximize his leverage. This is also a reason why the top of the sail needs to be depowered when planing upwind, to decrease the heeling moment produced by the sail. By depowering the sail and decreasing the sail angle of attack well below stall angle, the actual sail and fin lift are around half the maximum values shown in Table 11, so as to balance the sailor and rig righting moment.

With these limitations in mind, we can estimate the actual lift and heeling moments when sailing upwind with the centreboard down or retracted, as shown in Table 12.

	Displacement or marginal planing, centreboard down		Planing, centreboard up	
	Transverse lift	Heeling moment	Transverse lift	Heeling moment
Sailor and rig weight moment	0N	-420Nm (well below max)	0N	-1210Nm (max)
Hull buoyancy moment	0N	-300Nm	0N	0N
Fin and centreboard lift	-260N (well below stall)	120Nm	-450N (well below stall)	180Nm
Sail lift	260N (max)	600Nm (max)	450N (well below stall)	1030Nm

Table 12: Estimated actual values of transverse force (positive to leeward) and heeling moment about universal joint (positive to leeward)

7. PLANING CALCULATIONS

7.1 TWO-DIMENSIONAL THEORY

The following calculations are based on two-dimensional planing theory, originally developed by Maruo (1951) for planing surfaces of known wetted length. The planing theory assumes small free surface slope (i.e. small trim angle for flat surfaces), so that the free surface boundary conditions may be linearized. This results in a singularity at the forward stagnation point, and a thin splash projected forward ahead of the stagnation point. The wetted length is defined as the distance from the trailing edge to the stagnation point where the splash commences.

The theory was later modified (Oertel 1975) to develop inverse equations for the wetted length and trim angle as a function of the net vertical force and trim moment, which are the true input parameters. An efficient computational method for general rocker profiles was described in Tuck (1994), showing the calculation of wetted length, trim angle, pressure distribution and inviscid resistance. Empirical flat-plate results for viscous resistance are then used to calculate total resistance as a function of speed, loading and centre of pressure position.

Other important research on planing theory has included a three-dimensional theory for very high Froude number (Wang & Rispin 1971) and empirical planing prediction methods for boat hulls (Savitsky & Brown 1976, Savitsky et al. 2007).

Here we shall apply the methods of Tuck (1994) and Gourlay (1994) to the case of an RS:X sailboard planing upwind with the centreboard fully retracted, as shown in Figure 4 and Figure 8.

Since we are using a 2D theory, the vertical force must be specified per metre of board width. We use the standard board, rig and sailor weight (described in Section 5.4) of 110kg, together with the mean board width 0.77m over its length, to determine a two-dimensional hydrodynamic lift of 1400 Newtons per transverse metre.

The hydrodynamic centre of pressure beneath the board must be such that all pitch moments are in balance, as shown in Figure 8. Aerodynamic lift on the board is neglected. We assume that the standard sailor's weight (77.5kg inc. clothing) is centred at the rear footstrap, which is 0.3m forward of the board's trailing edge. In this position, the sailor is leaned slightly toward the back of the board, to balance the forward drive force produced by the rig.

The rig is raked aft at 20º to close the gap between the sail and board, and hence maximize the sail lift/drag ratio (Marchaj 1979). The universal joint may be shifted longitudinally in the mast track, so as to balance the longitudinal position of the sail lift centre and fin lift centre (as shown in Figure 7) and hence keep the board in balance. With the mast track set at the 3rd position forward (1.4m from the trailing edge), the 12.5kg rig centre of gravity sits 0.1m aft of the board's trailing edge. The 19.5kg board centre of gravity sits 1.4m forward of the trailing edge. Therefore the combined sailor, rig and board weight (110kg) is centred 0.35m ahead of the board's trailing edge.

An estimate of the sail drive force may be obtained by balancing it against the board and fin resistance. As we shall see, board hydrodynamic resistance is approximately 100N at the representative upwind board speed of 12 knots. With the fin operating at around half its maximum lift (see §5), and assuming a lift/drag ratio of 10, the total hydrodynamic resistance and hence sail drive is in the order of 150N.

Approximating the sail centre of effort at the rig centre of gravity (1.8m above the board in the raked-back position), the offset vertical distance between the sail drive and hydrodynamic resistance gives a bow-down pitching moment of 270Nm. This moment must be a balanced by a bow-up pitching moment caused by the offset longitudinal distance between the total weight force and hydrodynamic centre of pressure (Figure 8). Using the total weight force of 1080N at 0.35m forward of the trailing edge, the hydrodynamic centre of pressure on the board must lie 0.6m forward of the board's trailing edge.

The rocker line of the RS:X is approximately flat over the aft 1.3m of the board. As we shall see, the wetted length over the planing speed range is around 0.8m. Therefore the planing surface of the RS:X may be considered longitudinally flat.

7.2 PLANING THEORY RESULTS

Using the hydrodynamic lift and centre of pressure determined in Section 6.1 for a typical RS:X sailboard, the wetted length, trim angle and hydrodynamic resistance can be calculated (Tuck 1994, Gourlay 1994). These calculations assume smooth water and do not include the effect of waves.

With the hydrodynamic centre of pressure 0.6m forward of the trailing edge (i.e. the centreboard retracted and the sailor in the rear footstraps), the planing hump (Tuck 1994) occurs at a speed of 4.8 knots. At this

speed, the board is at its maximum trim angle, with large associated resistance. As the speed increases, the trim angle and inviscid resistance decrease quickly, and the board enters the pure planing regime, where the weight is supported by hydrodynamic lift rather than buoyancy forces. According to the Savitsky criteria (Savitsky & Brown 1976), this occurs at a speed of 8 knots for the RS:X, so we shall only provide planing results in excess of this speed. While this article concentrates on upwind sailing, at which the maximum board speed is 12 − 14 knots, we shall also provide results up to 24 knots, which is the maximum board speed consistently measured by the authors when broad reaching in strong winds.

The calculated bow-up trim angle of the board's planing surface is shown in Figure 9. This gives the angle of the flat planing surface above the horizontal, when the board is in equilibrium.

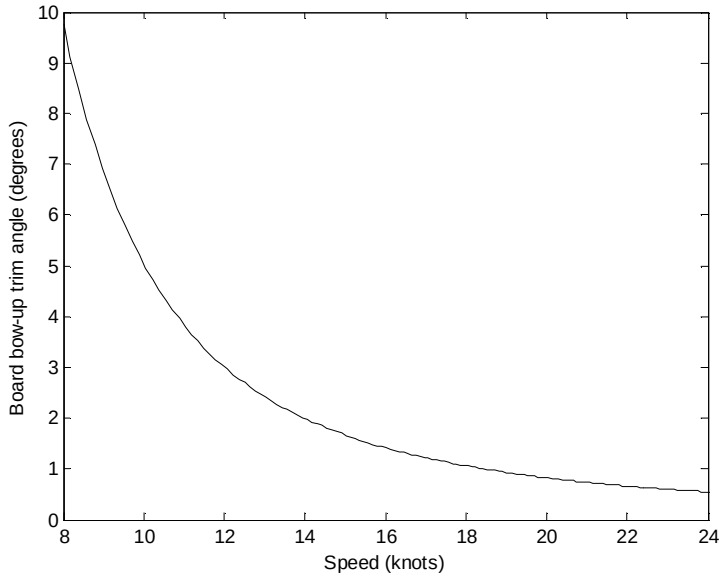

Figure 9: Board trim angle from planing theory

We see that a large trim angle is predicted at low speeds, when the board is just entering the planing regime. At 12 knots, the trim angle is 3º, decreasing to 2º at 14 knots. Therefore over the typical upwind speed range 12 − 14 knots, significant changes in trim occur due to board speed alone.

While the trim changes markedly with board speed, the wetted length remains approximately constant over the chosen speed range, at 1.3 times the hydrodynamic lift centre position, or 0.8m ahead of the trailing edge. The vertical position of the midpoint of the wetted length also remains approximately constant, at 0.01 − 0.03m above the still water level.

Hydrodynamic resistance of the board according to 2D planing theory is shown in Figure 10. The inviscid resistance is calculated from the horizontal pressure force component (Tuck 1994). The viscous resistance uses the calculated wetted length, together with a turbulent flat plate viscous resistance empirical estimate (White 1999, p442).

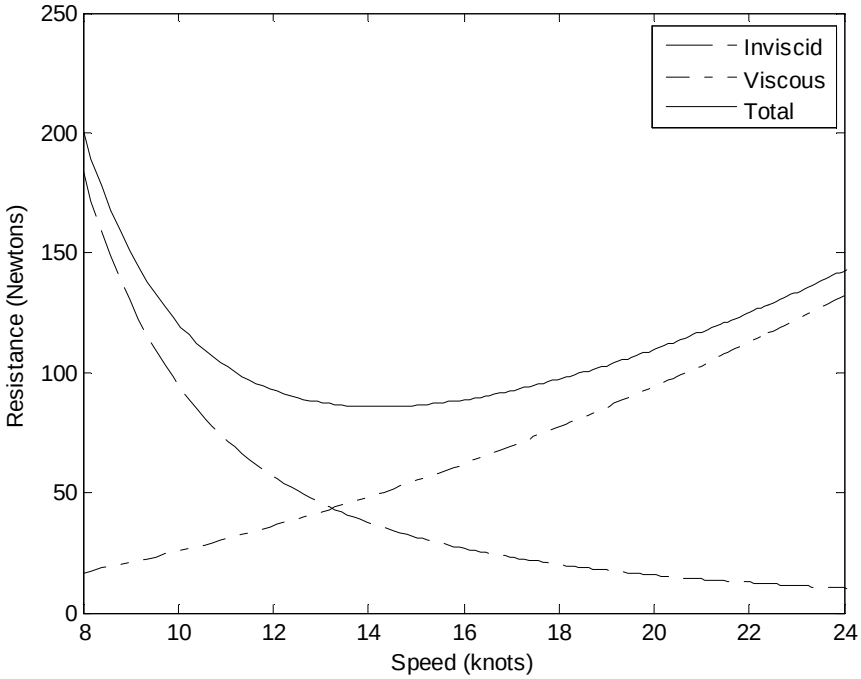

Figure 10: Board resistance (excluding fin) from planing theory

We see that the inviscid resistance decreases sharply as the speed increases, because the trim decreases and the board's planing surface comes closer to horizontal. It is this property of planing surfaces that allows them to operate efficiently at high speeds. The viscous resistance increases approximately with the speed squared, since the wetted length remains approximately constant.

The total resistance has a minimum at 13 − 15 knots. Note that these calculations are for the board only, and that the fin's resistance will increase with the speed squared and also be affected by the angle of attack. Therefore it appears that the normal upwind planing board speeds of 12 − 14 knots are close to the minimum of the total hydrodynamic resistance curve.

8. CONCLUSIONS

A sailboard planing upwind on a single fin represents a delicate force balance between sail lift, fin lift, planing lift and the sailor's weight. The nature of these forces has been discussed with reference to previous research on sailboards and related topics. Results have then been applied to the specific case of an RS:X Olympic sailboard.

The rig of an RS:X sailboard is quite rigid, due to the carbon mast and boom, coupled with high downhaul tension applied to the fully-battened sail. This locks in the sail shape, so that useful measurements of sail camber, twist and fore-aft mast bend may be made on land for different rig settings. These comparisons have been made for realistic rig settings, board speeds and headings. The large amounts of twist obtainable in the RS:X sail have been demonstrated and discussed with reference to the maximum righting moment able to be produced by the sailor's weight.

Force diagrams have been included for the hull, rig and sailor in each two-dimensional plane. Limiting forces and moments, as well as typical actual values, have been calculated for each of the external forces on the sailboard. Using a standard sailor's height and mass, it has been shown that the lift on the above-water and below-water foils are well balanced, and the sailor's weight is the major constraint on sail lift in planing conditions.

A two-dimensional planing analysis of the RS:X board has confirmed the typical upwind planing speed of 12 − 14 knots as a local minimum in the resistance curve. Board trim has been shown to change drastically over this and other speed ranges, while wetted length remains approximately constant.

9. ACKNOWLEDGEMENTS

The authors acknowledge the assistance of Fremantle Sailing Club and the ISAF Emerging Nations Program in conducting the experimental testing.

10. REFERENCES

ABBOTT, I.H., VON DOENHOFF, A.E., Theory of wing sections, including a summary of airfoil data, Dover Publications, New York, 1959.

AVILA, M.R., Computational and experimental investigation of the aerodynamic characteristics of a windsurfing sail section, Aeronautical and Astronautical Engineering thesis, Naval Postgraduate School, Monterey, 1992.

BROERS, C.A.M., CHIU, T.W., POURZANJANI, M.M.A., BUCKINGHAM, D.J., Effects of fin geometry and surface finish on sailboard performance and manoeuvrability, Manoeuvring and Control of Marine Craft (Ed. P.A. Wilson), Computational Mechanics Publications, 1992, 275 – 289.

CASTAGNA, O., VAZ PARDAL, C., BRISSWALTER, J., The assessment of energy demand in the new Olympic windsurf board: Neilpryde RS:X, 2007, Eur. J. Appl. Physiol. 100, 247–252.

CHIU, T.W., KALAUGBER, P.G., BROERS, C.A.M., The application of photogrammetry in the study of the effects of sailboard fin flexibility, Proc. Instn Mech. Engrs, 1995, Vol. 209, No. C6, 373 – 381.

DAY, A.H., Sail optimisation for maximal speed, Journal of Wind Engineering and Industrial Aerodynamics 63, 1996, 131-154.

GOURLAY, T.P., Planing, Hons. App. Maths. Thesis, University of Adelaide, 1994.

HANSEN, K., Analysis of flow around an RS:X Racing 66 windsurfing fin, Hons. Thesis, Dept. Imaging and Applied Physics, Curtin University, 2011.

INTERNATIONAL SAILING FEDERATION (ISAF) International RS:X class rules 2011, www.sailing.org.

KILLING, S., HUNTER, D., Yacht design explained, Norton Books, New York, 1998.

LUCIANI, L., Human Physiology, Vol. 3, MacMillan and Co., London, 1913.

MARCHAJ, C.A., Aero-hydrodynamics of sailing, Dodd, Mead & Co., New York, 1979.

MARTELLOTTA, J., Performance analysis of one design sailing dinghies through measurement of rig characteristics, B.Eng. thesis, Curtin University, 2010.

MARUO, H., Two-dimensional theory of the hydroplane, Proc. 1st Japan Nat. Congr. for Appl. Mech., Tokyo, 1951.

NEWMAN, J.N., Marine Hydrodynamics, 7th Ed., MIT Press, 1992.

OERTEL, R.P., The steady motion of a flat ship, including an investigation of the local flow near the bow, Ph.D. thesis, University of Adelaide, 1975.

PARTIDA, L.P., Comparative computational analysis of airfoil sections for use on sailing craft, Aeronautical and Astronautical Engineering thesis, Naval Postgraduate School, Monterey, 1996.

SAVITSKY, D., WARD BROWN, P., Procedures for hydrodynamic evaluation of planing hulls in smooth and rough water, Marine Technology, Vol. 13, No. 4, 361-400, 1976.

SAVITSKY, D., DELORME, M.F., DATLA, R., Inclusion of whisker spray drag in performance prediction method for high-speed planing hulls, Marine Technology, Vol. 44, No. 1, 35-56, 2007.

SWALES, P.D., WRIGHT, A.J., McGREGOR, R.C., ROTHBLUM, R.S., The mechanisms of ventilation inception of surface piercing foils, J. Mech. Eng Sci., 1974, Vol. 16, No. 1, 18 – 24.

TIMOSHENKO, S.P., GERE, J.M., Mechanics of materials, D. Van Nostrand Company, 1972.

TUCK, E.O., The planing splash, 9th Int. Workshop on Water Waves and Floating Bodies, Kuju, Japan, April 1994. Proc. Ed. M. Okhusu, Kyushu University, 217-220.

WALLS, J.T., GALE, T.J., A technique for the assessment of sailboard harness line force, Journal of Science and Medicine in Sport 4(3): 348-356, 2001.

WANG, S., ZHAO, L., LI, D., The aerodynamic performance analyses of windsurfing pumping based on dynamic mesh, Acta Aerodynamica Sinica, 2009, Vol. 2009-04 (in Chinese).

WANG, D.P, RISPIN, P., Three-dimensional planing at high Froude number, Journal of Ship Research, Vol. 15, 1971.

WHITE, F.M., Fluid Mechanics, 4th Ed., McGraw-Hill, 1999.